Biogeosciences, 11, 6755–6768, 2014
www.biogeosciences.net/11/6755/2014/
doi:10.5194/bg-11-6755-2014

Biogeosciences
Open Access

Dependence of the cyclization of branched tetraethers on soil moisture in alkaline soils from arid–subhumid China: implications for palaeorainfall reconstructions on the Chinese Loess Plateau

H. Wang[1,2], W. Liu[1,3], and C. L. Zhang[4]

[1]State Key Laboratory of Loess and Quaternary Geology, IEE, CAS, Xi'an, 710075, China
[2]University of Chinese Academy of Sciences, Beijing 100049, China
[3]School of Human Settlement and Civil Engineering, Xi'an Jiaotong University, Xi'an 710049, China
[4]State Key Laboratory of Marine Geology, Tongji University, Shanghai 200092, China

Correspondence to: W. Liu (liuwg@loess.llqg.ac.cn) and C. L. Zhang (archaeazhang_1@tongji.edu.cn)

Received: 11 January 2014 – Published in Biogeosciences Discuss.: 27 June 2014
Revised: 25 October 2014 – Accepted: 27 October 2014 – Published: 8 December 2014

Abstract. The use of branched glycerol dialkyl glycerol tetraethers (bGDGTs) in loess–palaeosol sequences (LPSs) has shown promises in continental palaeotemperature reconstructions. Thus far, however, little is known about the effect of soil moisture on their distributions in the water-limited Chinese Loess Plateau (CLP). In this study, the relationships between environmental variables and the cyclization of branched tetraethers (CBT) were investigated in arid–subhumid China using 97 surface soils in the CLP and its vicinity, as well as 78 soils with pH > 7 which have been previously published. We find that CBT correlates best with soil water content (SWC) or mean annual precipitation (MAP) for the overall data set. This indicates that CBT is mainly controlled by soil moisture instead of soil pH in alkaline soils from arid–subhumid regions, where water availability is a limiting factor for the producers of bGDGTs. Therefore, we suggest that CBT can potentially be used as a palaeorainfall proxy on the alkaline CLP. According to the preliminary CBT–MAP relationship for modern CLP soils (CBT $= -0.0021 \times$ MAP $+ 1.7$, $n = 37$, $r = -0.93$), palaeorainfall history was reconstructed from three LPSs (Yuanbao, Lantian, and Mangshan) with published bGDGT data spanning the past 70 ka. The CBT-derived MAP records of the three sites consistently show precession-driven variation resembling the monsoon record based on speleothem δ^{18}O, supporting CBT as a reasonable proxy for palaeorainfall reconstruction in LPS. The direct application of CBT as a palaeorainfall proxy in corroboration with the bGDGT-based temperature proxy may enable us to further assess the temperature/hydrological association for palaeoclimate studies on the CLP.

1 Introduction

The deposits of wind-blown dust (i.e. loess) on the Chinese Loess Plateau (CLP; Fig. 1) are natural archives of past climate change. Characteristically, the plateau consists of a sequence of alternating loess and palaeosol layers, which have accumulated at least since 2.6 Ma BP (before present; Liu, 1985; Liu and Ding, 1998), with the records extending back to late Oligocene (Heller and Liu, 1982; Guo et al., 2002; Qiang et al., 2011). The cyclic alternation of loess and palaeosol provides highly visible records of regional climate history resulting from changing monsoon intensity on glacial–interglacial timescales (An, 2000, and references therein; Porter, 2001). For the past 3 decades, numerous proxies have been shown to be indicative of monsoon intensity in loess–palaeosol sequences (LPSs), including the traditional pedogenic magnetic susceptibility (e.g. Liu, 1985; Zhou et al., 1990; Maher et al., 1994) and grain size distributions (e.g. Ding, 1994; Sun et al., 2006), the geochemistry of iron oxides (e.g. Ding et al., 2001), the δ^{18}O of rhizoconcretions and land snail shells (Li et al., 2007), the δ^{13}C of total organic matter (An et al., 2005; Liu et al., 2005a, b; Ning et al., 2008; Rao et al., 2013) or carbonate (Liu et al., 2011), the

Published by Copernicus Publications on behalf of the European Geosciences Union.

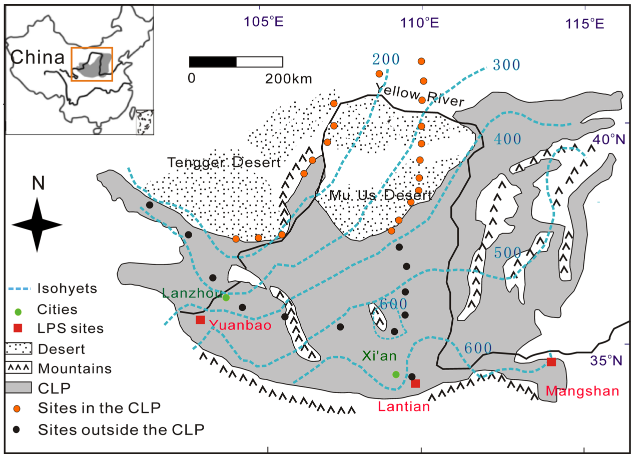

Figure 1. Sketch map of the CLP and its surroundings showing the location of sampling sites for surface soils collected in this study (modified from Xia et al., 2012). The sites of three LPS sections with published bGDGT data (Yuanbao, Lantian and Mangshan) are also shown. The relative position of the study region in China is indicated in the upper left.

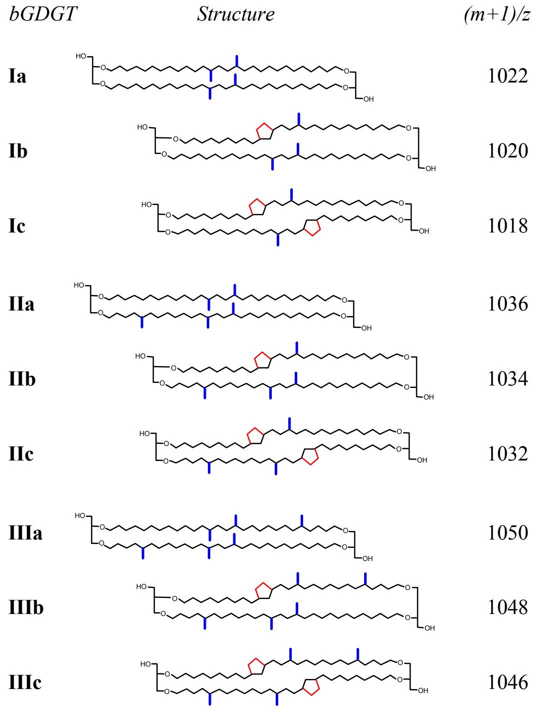

Figure 2. Molecular structures of bGDGTs and the mass to charge ratios of protonated molecular ions (after Weijers et al., 2007a).

δ^{13}C and δD of leaf wax *n*-alkanes (Zhang et al., 2003, 2006; Liu and Huang, 2005; Liu et al., 2005b), phytolith (Lu et al., 2006, 2007), and trace metal ratios (Li and Li, 2014). However, since many proxies suffer from inherent weaknesses such as uncertainties of interpretation (e.g. controversy of precipitation-controlled vs. temperature-controlled) or sample unavailability (Yang et al., 2014a), the development of new palaeoclimatic proxies specific for temperature or precipitation is still necessary for this climatologically important region.

Recent advances in analytical methods using high-performance liquid chromatography (HPLC)–mass spectrometry (MS) techniques enabled the identification of a range of new lipid biomarkers – glycerol dialkyl glycerol tetraethers – GDGTs (Hopmans et al., 2000; Sinninghe Damsté et al., 2000), as well as the subsequent understanding of their environmental occurrence and geochemical importance (reviewed in Schouten et al., 2013a). Particularly, the branched GDGTs (bGDGTs; Fig. 2) are ubiquitous in soils (Hopmans et al., 2004; Weijers et al., 2006a, 2007a; Sinninghe Damsté et al., 2008; Tierney and Russell, 2009; Peterse et al., 2009a, b, 2012; Huguet et al., 2010; Loomis et al., 2011; Tierney et al., 2012; Yang et al., 2012, 2014a; Wang et al., 2013; Liu et al., 2013). They are presumed to originate from the cell membranes of unknown bacterial species (Weijers et al., 2006b; Sinninghe Damsté et al., 2011) with a heterotrophic lifestyle (Pancost and Sinninghe Damsté, 2003; Oppermann et al., 2010; Weijers et al., 2010). By the study of bGDGT distributions in > 130 globally distributed soils, Weijers et al. (2007a) found that the relative extent of cyclopentane moieties, expressed as the cyclization ratio of branched tetraethers (CBT), is negatively correlated to soil pH, whereas the degree of methylation for the nine bGDGTs, expressed as the methylation index of branched tetraethers (MBT), is positively correlated with the mean annual air temperature (MAAT) and to some extent to soil pH. Therefore, palaeosoil pH and MAAT can be quantified using CBT and the combination of MBT and CBT (MBT/CBT), respectively (Weijers et al., 2007a).

An extended survey of 278 globally distributed surface soils further confirmed that CBT relates best to soil pH, while the simplified form of MBT (i.e. MBT' based on the seven most common bGDGTs) and CBT were shown to correlate with MAAT ($R^2 = 0.59$, RMSE = 5.0 °C; Peterse et al., 2012). Yang et al. (2014a) further investigated the distribution of GDGTs in > 100 surface soils across a large climatic gradient of China, and proposed an alternative transfer function for MAAT reconstruction based on the fractional abundances of bGDGTs for use in arid/semiarid regions. This calibration applies a stepwise selection method (SSM) and has a higher determination factor ($R^2 = 0.87$) and lower root mean square error (RMSE = 1.7 °C) in Chinese soils than the local MBT/CBT proxy calibration ($R^2 = 0.86$, RMSE = 1.8 °C; Yang et al., 2014a). Recently, however, De Jonge et al. (2013) identified a new set of bGDGT isomers for hexamethylated bGDGTs and pentamethylated bGDGTs, the so-called 6-methyl bGDGTs, which co-elute with 5-methyl bGDGTs that are used to calculate the CBT and MBT' indices commonly used so far. Further separation of bGDGTs using an improved chromatographic method showed that the presence of 6-methyl bGDGTs may introduce scatter in the relationships between previous bGDGT indices and MAAT and pH. Hence, new indices with improved soil pH and MAAT estimates, i.e. the CBT' comprising the 6-methyl bGDGTs and the MAT_{mr} – a multiple linear regression, might be more promising for accurate palaeoclimate reconstructions (De Jonge et al., 2014).

The sensitivity of soil bGDGT distribution to environmental variation offers new tools to quantitatively infer past continental climate change in LPS. Initial application of the bGDGT palaeothermometer to LPSs from the Mangshan (Peterse et al., 2011, 2014), Lantian (Gao et al., 2012), Yuanbao (Jia et al., 2013), and Weinan (Yang et al., 2014a, b) sections on the CLP indicates that bGDGTs might have recorded past changes in air temperature driven by local solar insolation. Unexpectedly, however, the CBT-reconstructed pH is lower for loess than for palaeosols (Jia et al., 2013; Peterse et al., 2014), in contradiction with the well-accepted view that loess formed under drier climate conditions and should be more alkaline. In fact, Xie et al. (2012) and Yang et al. (2014a) have recently observed a negative correlation between CBT and soil pH when pH is < 7, but a slightly positive correlation between CBT and soil pH or flattening off of CBT with increasing pH when pH is > 7, implying that some other factor(s) may play a role in the cyclization of bGDGTs in alkaline soils. Based on the negative CBT–MAAT correlation in their studied alkaline soils, Yang et al. (2014a) proposed that temperature is possibly the dominant factor controlling the cyclization of bGDGTs in these environments; but this remains to be tested due to the covariation between MAP and MAAT in their data set.

Water availability is important in affecting the distribution of bGDGTs in modern soils (Loomis et al., 2011; Peterse et al., 2012; Dirghangi et al., 2013; Menges et al., 2014). This might be particularly true for soils in water-limited environments (arid, semiarid, and subhumid regions) where soil moisture or mean annual precipitation (MAP) has been found to influence MBT' and may lead to a "cold bias" of reconstructed MAAT based on the MBT' / CBT index (Peterse et al., 2012; Dirghangi et al., 2013; Menges et al., 2014). Until now, however, the effect of soil moisture on the CBT index has rarely been explored in alkaline soils from water-limited regions. In the present study, therefore, we analysed the distribution of bGDGTs in the CLP and the adjacent arid/semiarid areas using 97 surface soils. Combining them with recently reported bGDGT data in 78 other Chinese soils with pH values > 7 (Xie et al., 2012; Yang et al., 2012, 2014a), we aimed to understand the environmental controls on the CBT index in alkaline soils in arid–subhumid China and ultimately to evaluate if CBT can be used as a direct proxy for palaeorainfall reconstruction in LPS.

2 Material and methods

2.1 Regional setting and sample collection

The CLP is the largest region of loess deposits in the world. It is characterized by temperate semiarid and subhumid climate, modified by latitude, longitude, and terrain. Both the MAAT and the MAP show a clear decrease northwestward (Fig. 1). Dominated by the strength of the East Asian summer monsoon (EASM) system, the precipitation occurs mostly in the summer months (from May to September), which accounts for approximately 68–87 % of the total annual precipitation (Ding, 1994; Liu et al., 2005a). The present-day CLP is mainly covered by shrub (e.g. *Sophora viciifolia and Vitex chinensis*) and grasses (e.g. *Artemisia* and Gramineae) (Liu, 1985). In general, the vegetation progressively becomes sparser and less dense from southeast to northwest, resulting from increasing dryness (Liu et al., 2005c).

A total of 97 samples were collected in late September, 2012, from 33 sites in the CLP and the surrounding areas (Fig. 1, Supplement Table 1). For each site, 2–5 samples were collected at locations tens to hundreds of metres apart, except for site DengkouB with only one sample being collected. Samples from the CLP (WLPS-1–WLPS-18 and WLPS-79–WLPS-97, totaling 37 samples) were collected from natural grassland or grassland that has been in restoration for > 10 a. At each sampling location, three randomly collected samples were pooled and mixed to make one composite sample representing that location. Most samples were collected from the uppermost layer of soil with a depth of less than 5 cm and they were transported to the laboratory immediately after collection and stored at -20 °C. The details of the samples are provided in the Supplement Table 1.

2.2 Environmental parameters

The SWC (soil water content) of the soils was obtained by weighting the sample before and after freeze-drying it.

Soil pH was measured following Wang et al. (2012): ca. 4 g of freeze-dried sample was added in 10 mL of distilled water; the mixture was stirred for 1 min, left to stand for 30 min, and pH of the supernatant was measured with a Sartorius PB-10 pH meter. The standard deviation for triplicate measurements was ± 0.03.

The meteorological data for our sampling sites were obtained from the China Meteorological Data Sharing Service System (http://cdc.cma.gov.cn/). For each sampling site, MAP, MAAT, mean annual ground surface temperature (MAGST), mean annual relative humidity (MARH) and mean annual evaporation (MAE) were generally estimated from the nearest weather station. However, if there were 2–3 stations nearby, the meteorological data from all of them were averaged for the sampling site. A further correction to the meteorological MAGST and MAAT values for each sample was made according to a lapse rate of -0.6 °C/100 m.

Table 1. Correlations between the distribution of bGDGTs (fractional abundances, CBT and MBT') and environmental variables (MAAT, MAP and soil pH) for the Chinese alkaline soils ($n = 165$) compiled in Yang et al. (2014a) and this study, with significant correlations ($p < 0.05$) indicated in bold.

		IIIa	IIIb	IIIc	IIa	IIb	IIc	Ia	Ib	Ic	CBT	MBT'
Soil pH	*r*	0.12	**−0.29**	**−0.19**	**0.26**	**−0.19**	−0.08	−0.13	**−0.24**	**−0.23**	**0.22**	**0.22**
	p	0.13	0.00	0.01	0.00	0.02	0.32	0.10	0.00	0.00	0.01	0.01
MAP	*r*	**−0.56**	**0.50**	**0.48**	**−0.78**	**0.69**	**0.56**	**0.51**	**0.81**	**0.70**	**−0.74**	**0.76**
	p	0.00	0.00	0.00	0.00	0.00	0.00	0.00	0.00	0.00	0.00	0.00
MAAT	*r*	**−0.61**	**0.28**	**0.42**	**−0.63**	**0.53**	**0.48**	**0.60**	**0.74**	**0.63**	**−0.59**	**0.76**
	p	0.00	0.00	0.00	0.00	0.00	0.00	0.00	0.00	0.00	0.00	0.00

2.3 Analysis of bGDGTs

The freeze-dried and homogenized samples (30–50 g) were extracted (4 × 10 min) with dichloromethane (DCM) : methanol (9 : 1, v/v) using an accelerated solvent extractor (ASE 350, Dionex) at 100 °C and 1500 psi. The total extract was dried under N_2 in a water bath. A known amount of C_{46} GDGT internal standard (IS; Huguet et al., 2006) was then added to the extract, which was redissolved in DCM : methanol (9 : 1, v/v) and divided into two halves. One half was dried under N_2, redissolved in hexane/isopropanol (99 : 1, v/v) and filtered over a 0.45 µm PTFE (polytetrafluoroethylene) filter.

An aliquot (10 µL) of sample was injected for HPLC-atmospheric pressure chemical ionization (APCI)-MS analysis according to a procedure slightly modified from Schouten et al. (2007) and Zhang et al. (2012). Separation of bGDGTs was achieved on an Alltech Prevail Cyano column (150 mm × 2.1 mm, 3 µm). The elution gradient was isocratic (5 min) at 99 % hexane / 1 % isopropanol followed by a linear gradient to 1.8 % propanol in 45 min. After each analysis, the column was cleaned by back-flushing using 90 % hexane / 10 % propanol. The flow rate was set at 0.2 mL min^{-1}. In order to increase sensitivity and reproducibility, selective ion monitoring (SIM) mode of the $[M+H]^+$ (protonated molecular ion) of the different bGDGTs (Fig. 2) was used to detect and quantify them. Quantification of each bGDGT was achieved by calculating the peak area in the chromatogram and comparing it with that of the IS. Ionization efficiency for bGDGTs and the IS was assumed identical.

The CBT index was calculated following Weijers et al. (2007a):

$$\text{CBT} = -\log((\text{Ib} + \text{IIb})/(\text{Ia} + \text{IIa})). \quad (1)$$

The MBT' index was calculated according to the following equation (Peterse et al., 2012):

$$\text{MBT}' = (\text{Ia} + \text{Ib} + \text{Ic})/(\text{Ia} + \text{Ib} + \text{Ic} + \text{IIa} + \text{IIb} + \text{IIc} + \text{IIIa}). \quad (2)$$

The MBT' / CBT-derived MAAT and MBT' / pH-derived MAAT was calculated as follows (Peterse et al., 2012):

$$\text{MAAT} = 0.81 - 5.67 \times \text{CBT} + 31.0 \times \text{MBT'}, \quad (3)$$

$$\text{MAAT} = -23.20 + 2.86 \times \text{pH} + 33.71 \times \text{MBT'}. \quad (4)$$

MAAT was also estimated using the Chinese SSM calibration model based on the fractional abundance of bGDGTs (Yang et al., 2014a):

$$\text{MAAT} = 20.9 - 13.4 \times \text{IIa} - 17.2 \times \text{IIIa} - 17.5 \times \text{IIb} + 11.2 \times \text{Ib}. \quad (5)$$

2.4 Soil data set compilation

In addition to the soils newly collected in the CLP and the surrounding areas in this study, we included other alkaline (pH > 7) soil samples in China with published bGDGT data available to generate the largest possible data set for determining the environmental controls on the distribution of bGDGTs in Chinese alkaline soils (Supplement Table 1). This combined data set consisted of 97 soils analysed in this study, 37 soils in Xie et al. (2012) and Yang et al. (2012), and 41 soils in Yang et al. (2014a). The MAP, pH and MAAT ranges for this data set are 7.2–9.2, 140–1138 mm, and 3.8–16.8 °C, respectively. Two soils (XJBC-3 and XJBC-5) of Yang et al. (2014a) collected at the northwestern margin of the Taklimakan Desert were not included in the data set because they were likely from the wet sites with surface/groundwater supply, and may not represent typical soils with a MAP of ca. 60 mm.

2.5 Statistical analyses

We performed a redundancy analysis (RDA) on the combined data set to visualize the environmental controls on the variation in fractional abundances of bGDGTs in Chinese alkaline soils employing the software Canoco for Windows 4.5 (ter Braak and Smilauer, 2002). According to previous studies (Peterse et al., 2012; Yang et al., 2014a), MAP, soil pH and MAAT are set as environment data while species data are the fractional abundances of individual bGDGTs. Detrended correspondence analysis (DCA) on the fractional abundances of bGDGTs showed that the gradient length was 1.4, much lower than 3 (ter Braak, 1988; ter Braak and Prentice, 1988; Yang et al., 2014a). Therefore, variability in the bGDGTs was linear and RDA was appropriate in this case.

The Pearson correlation coefficients between environmental variables and bGDGT distributions were determined with the Windows SPSS 16.0 software program. We accepted a p value of < 0.05 as being significant.

3 Results and discussion

3.1 Statistical results

The results of the RDA show that the first two RDA axes cumulatively explained 51.9 % of the bGDGT distribution data and 99.9 % of the relationships between bGDGTs and environmental factors. The first axis (axis 1) alone explains 50.3 % of the variance of bGDGT distribution and captures the gradients in MAP and MAAT. However, the correlation coefficient of axis 1 and MAP is 0.81, higher than that for axis 1 and MAAT (0.74). Soil pH correlates more weakly ($r = -0.24$) with axis 1. In addition, based on the angles between the fractional abundances of bGDGTs and environmental factors, the relative abundances of bGDGTs with a high degree of cyclization (Ib, Ic, IIb, IIc, IIIb and IIIc) correlate positively with MAP (Fig. 3). For acyclic bGDGTs, Ia varied positively with MAAT and MAP, whereas IIa and IIIa varied negatively with MAAT and MAP.

The relationships between bGDGT distributions and environmental variables (i.e. pH, MAP and MAAT) can be further demonstrated by the correlation coefficients calculated by SPSS (Table 1). As expected, each individual bGDGT correlates significantly ($p < 0.01$) with MAP and MAAT, with the correlation coefficients much higher than those with soil pH (except for IIIb exhibiting the weakest correlation with MAAT). For the proportions of cyclic bGDGTs and acyclic bGDGT IIa, they are most closely related to MAP ($r = 0.81$, 0.70, 0.69, 0.56, 0.50, 0.48 and -0.78 for Ib, Ic, IIb, IIc, IIIb, IIIc and IIa, respectively). For the proportions of acyclic Ia and IIIa, they are most closely related to MAAT ($r = 0.60$ for Ia and -0.61 for IIIa). These are in agreement with the visualized RDA results (Fig. 3). Moreover, the MBT index representing the degree of methylation for bGDGTs correlates significantly ($p < 0.01$) with both MAAT ($r = 0.76$) and MAP ($r = 0.76$), while the CBT index expressing the relative extent of cyclopentane moieties in bGDGTs is most related to MAP ($r = -0.74$, $p < 0.01$) and to a lesser extent to MAAT ($r = -0.59$, $p < 0.01$).

3.2 Insensitivity of CBT to soil pH variation in alkaline soils

For the Chinese alkaline soil data set, pH seems unaccountable for the variance in the distribution of bGDGTs (Fig. 3)

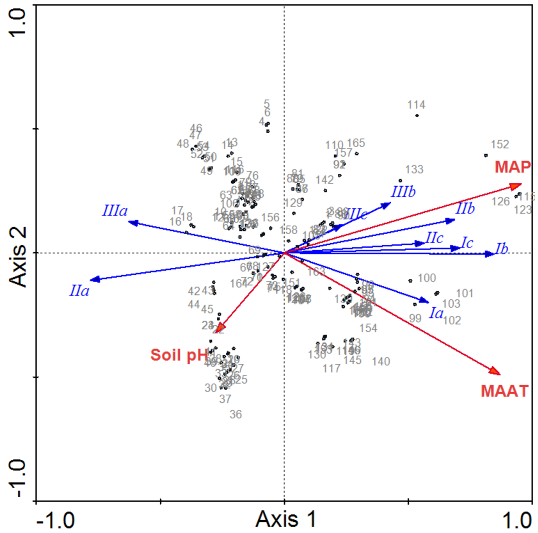

Figure 3. RDA triplot showing the relationships between environmental variables (red arrows) and fractional abundances of the nine bGDGTs (blue arrows) for the 165 Chinese alkaline soil samples compiled in Yang et al. (2014a) and in this study. Numbers refer to samples listed in Supplementary Table 1.

and there is only a slightly positive relationship between CBT and pH (Table 1 and Fig. 4; $r = 0.22$, $p = 0.01$, $n = 165$). This seems different from previous regional or global soil investigations at a large pH range, which have showed a strong positive control of pH on the relative abundance of bGDGTs containing cyclopentyl rings and thus CBT correlated negatively with pH (Weijers et al., 2007a; Peterse et al., 2009b, 2012; Menges et al., 2014). However, we note that the proportion of alkaline soils is relatively small in each soil sample set of the aforementioned studies. In fact, by extending the pH to > 9, Xie et al. (2012) and Yang et al. (2014a) have pointed out that the CBT index appears to be unable to distinguish pH variation, due to the weak positive CBT–pH relationship or a flattening off of CBT when the pH is > 7, despite that the CBT values still exhibit a significant ($p < 0.01$) negative correlation with soil pH when pH is < 7 (Fig. 4). The flattening off of CBT at higher soil pH values is also observed by Peterse et al. (2010), who analysed bGDGTs in long-term soil pH manipulation plots in Scotland. Moreover, in lacustrine systems, a seemingly similar pattern also exists in the surface sediments of 23 lakes in China and Nepal (Sun et al., 2011), as well as in suspended particulate matter (SPM) from 23 lakes in the USA (Schoon et al., 2013). The weak correlation between CBT and pH under alkaline conditions suggests that variation in CBT might be problematic for tracing pH variation in alkaline soils.

The insensitivity of CBT to soil pH variation in alkaline soils might be caused by the inaccurate identification and subsequent quantification of 5-methyl bGDGTs. It has been observed that higher pH may decrease the fractional abun-

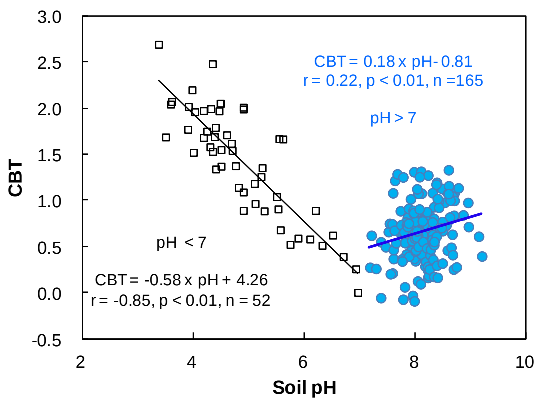

Figure 4. Plot of soil pH vs. CBT for the Chinese alkaline soils used in this study (indicated by blue solid circles), with previously published data from Yang et al. (2012), Xie et al. (2012), and Yang et al. (2014a). Also shown is the correlation between pH and CBT in other Chinese soils with pH < 7 (Weijers et al., 2007; Xie et al., 2012; Yang et al., 2012, 2014a).

dances of 5-methyl IIa but increase the fractional abundances of 6-methyl IIa in globally distributed soils (De Jonge et al., 2014). Since the two isomers are regarded as "normal" IIa (which is positively correlated with pH) in the calculation of CBT (which is negatively correlated with pH) using the traditional HPLC method (Weijers et al., 2007a), the CBT values would be overestimated if 6-methyl IIa exists. The exclusion of 6-methyl bGDGTs in the CBT index (defined as CBT_{5ME}), however, exhibits only slight improvement in relation to soil pH when pH is > 7 for the global soil data set (De Jonge et al., 2014). Therefore, De Jonge et al. (2014) further defined a new proxy for soil pH reconstruction, the so-called CBT' index, which comprises the pH-dependent 6-methyl bGDGTs and separates the opposite relations of 6-methyl IIa and 5-methyl IIa with pH. It correlates strongly with pH in globally distributed soils, with the RMSE (root mean square error) of the subset of arid soils decreasing from 2.9 to 0.3 pH units (De Jonge et al., 2014). The newly proposed CBT' index seems more promising for pH reconstruction in palaeoclimate studies, particularly in arid and alkaline soils.

Alternatively, the absence of a clear CBT–pH relationship under alkaline conditions possibly reflects that a certain threshold is reached for bGDGT producers in adapting their membrane lipids to pH. For the global soil data set, the correlations between the relative abundance of cyclic 5-methyl bGDGTs (e.g. Ib and IIb) and pH are indeed very weak under alkaline conditions (De Jonge et al., 2014). Previously, Weijers et al. (2007a) proposed two likely mechanisms for the negative CBT–pH relationship when pH is < 7. Firstly, it is important for the microbes to keep the internal pH constant within the cell, and therefore the bGDGT-producing bacteria tend to reduce the production of cyclopentyl moieties (causing higher CBT) at lower pH for better membrane packing and lower membrane permeability, which helps to protect cells against low pH (Weijers et al., 2007a). When pH is > 7, however, there seems to be no need for soil bacteria to overcome the inhibition of acidity. Secondly, the proton permeability (i.e. the pH gradient) of the cell membrane plays a crucial role in driving energy reactions over the cell membrane (e.g. Booth, 1985). Introduction of cyclopentyl moieties would allow more water molecules to get trapped in the membrane and consequently increase the membrane proton permeability, whereas a steeper proton gradient (thus lower ambient pH) is counteracted by a more impermeable membrane resulting from fewer cyclopentyl moieties and thus higher CBT (Weijers et al., 2007a). Under alkaline conditions, however, further adaptation of the cell membrane would not be needed to overcome H^+ leakage (Schoon et al., 2013) if the bGDGT producers turn to use Na^+ for energy transduction as neutrophiles and alkaliphiles, which are able to perform energy transduction by establishing a Na^+ gradient in combination with an H^+ gradient (Speelmans et al., 1995; Schoon et al., 2013). These mechanisms could possibly explain the apparent insensitivity of CBT to pH in alkaline conditions theoretically. Hence, variation in CBT values should be attributed as a response to other factor(s) for the alkaline soils.

3.3 Sensitivity of CBT to soil moisture in alkaline soils

Soil moisture can potentially affect the distribution of bGDGTs in modern soils (Loomis et al., 2011; Peterse et al., 2012; Dirghangi et al., 2013; Menges et al., 2014). SWC is a direct measurement of soil moisture. Notably for our soils collected in the CLP and its adjacent arid/semiarid areas, the CBT index correlates more strongly with SWC ($r = -0.67$, $p < 0.01$, $n = 97$; Fig. 5a) than with soil pH ($r = 0.50$, $p < 0.01$, $n = 97$; Fig. 5b), pointing to a likely negative control of soil moisture on the CBT index in alkaline soils in the water-limited regions. Some of the scatters in the SWC–CBT relationship might be due to that our measured SWC is an instantaneous value that is liable to differences in local rainfall for different sites and may not accurately represent the average soil moisture condition during the growth of bGDGT producers. For instance, soils at site Yongdeng (MAP: 284 mm) should be drier than those at the adjacent site Gulang (MAP: 352 mm). However, the measured SWC values for soils in Yongdeng (13, 13, and 12 %) collected immediately after a rainfall (according to our field note) were much higher than those for Gulang (3, 6, and 3 %). In such a case, the use of SWC at this sampling time could lead to an overestimation of the effect of soil moisture availability on bGDGT producers in Yongdeng (Fig. 5a). Omitting the Yongdeng samples, the CBT–MAP relationship was improved ($r = -0.75$). For extensive surface soil investigations, therefore, variation in SWC at the time of sampling can only roughly reflect differences in mean soil moisture conditions.

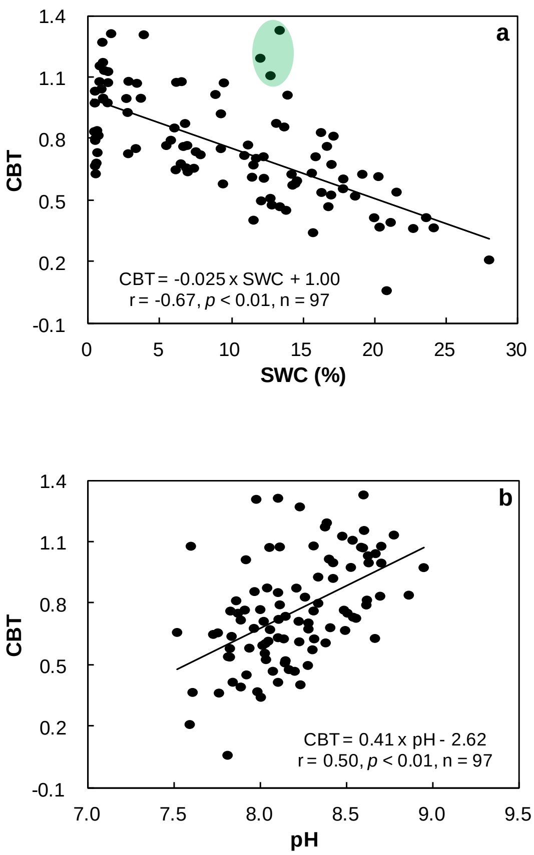

Figure 5. Linear regression plots of **(a)** CBT vs. SWC and **(b)** CBT vs. pH for 97 surface soils in this study. The light green shade in **(a)** indicates three Yongdeng soil samples collected immediately after a rainfall.

In contrast, MAP data would be more representative of the mean soil moisture than the instantaneous SWC value when continuous local soil moisture observation data were not available. Therefore, the MAP that is generally available in the data sets of previous studies is used to represent soil moisture in further discussions. As is expected, amongst the three environmental variables (MAAT, MAP, and soil pH) MAP is the dominant one that affects the relative abundance of cyclic bGDGTs with cyclopentyl moieties and thus the CBT index for the Chinese alkaline soils (Fig. 3, Table 1), further supporting soil moisture as the dominant environmental control on the CBT index in alkaline soils.

It might be argued that the negative MAP–CBT relationship (Fig. 6a) is possibly an artifact of CBT and MAAT being negatively correlated (Fig. 6b) and MAP and MAAT being intercorrelated (Fig. 6c). However, the correlation of MAP–CBT is stronger than that of MAAT–CBT ($r = -0.74$ for MAP–CBT and -0.59 for MAAT–CBT; Table 1), particularly when only considering the soils newly collected in this study ($r = -0.72$ for MAP–CBT and -0.28 for MAAT–CBT, $n = 97$; Fig. 6a, b). Moreover, we observed that the negative relationship between MAP and CBT is also significant ($p < 0.01$) in alkaline soils of two other regional data sets that show no MAAT–CBT correlation (in the USA: $r = -0.80$ for MAP–CBT and 0.26 for MAAT–CBT; Fig. 6d, e; De Jonge et al., 2014) or inverse MAAT–CBT correlation (across the Iberian Peninsula: $r = -0.65$ for MAP–CBT and 0.59 for MAAT–CBT; Fig. 6g, h; Menges et al., 2014). The results of these studies in different regions collectively suggest that the negative correlation between CBT and MAP might be valid for alkaline soils in water-limited regions, despite that the influence of temperature on CBT cannot be excluded at present.

The reason why CBT correlates with soil moisture in alkaline soils in arid–subhumid regions remains speculative as the exact biological source of bGDGTs is unknown. A likely explanation for the positive correlation between MAP and the relative abundance of cyclic bGDGTs (and thus the negative MAP–CBT relationship) might be that, under drier conditions, a more dense packing of membrane lipids is needed for bGDGT-producing organism(s) to avoid overevaporation of intracellular water. As a result, the formation of cyclopentyl moieties, which could result in loosening of the packing of the membrane lipids (Weijers et al., 2007a), is inhibited in soils at lower MAP values. Another possible reason for the MAP–CBT relationship in alkaline soils in water-limited regions might be a response of the community change of bGDGT producers with different soil moisture conditions; however, we currently know nothing about what organism(s) would produce more acyclic bGDGTs in drier soils under alkaline conditions. Further studies are needed to explore the exact underlying mechanism responsible for the observed moisture dependence of the CBT index in alkaline soils from arid–subhumid regions.

It should be noted that we only suggest the relation between CBT and soil moisture valid in alkaline soils from arid–subhumid regions. There is no evidence for a strong relation between soil moisture and CBT over the whole pH range of the global calibration set (De Jonge et al., 2014) or other regional data sets (e.g. Menges et al., 2014; Yang et al., 2014a). In fact, both pH (Weijers et al., 2007) and soil moisture (as discussed previously) might be important in controlling the membrane lipid composition of soil bGDGT producers. In humid regions where water availability is not a limiting factor, changes in soil pH might dominate the variations in CBT values (Weijers et al., 2007; Peterse et al., 2012). In contrast, water availability is generally a limiting factor for the growth of microorganisms in soils from arid–subhumid regions (e.g. Wang et al., 2013; Menges et al., 2014). Since it seems that CBT is insensitive to soil pH in alkaline soils (Xie et al., 2012; Yang et al., 2014a and Sect. 3.2), variations in CBT might be predominantly controlled by changes in soil moisture. In acid soils in arid–subhumid regions, however, both pH and soil moisture can influence the CBT values. Therefore, we tentatively restrict the CBT–soil moisture relationship to alkaline soils from arid–subhumid regions.

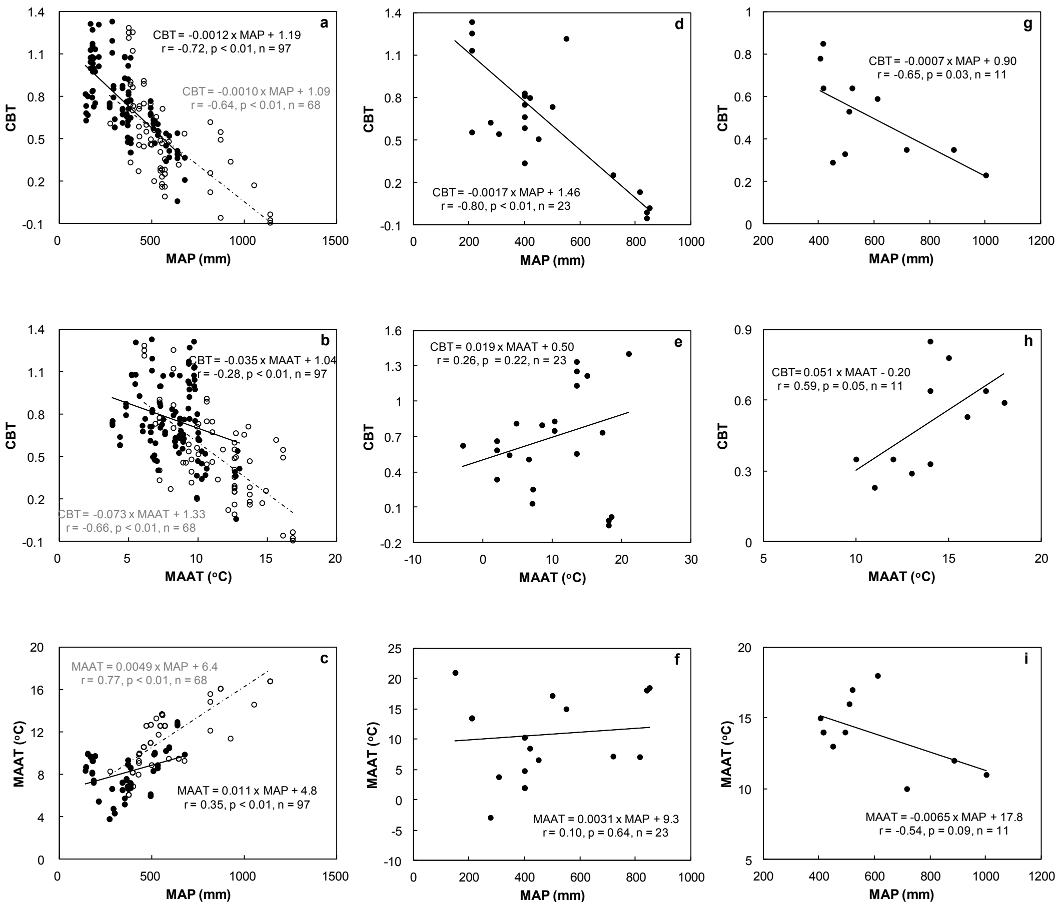

Figure 6. Plots showing the correlations of CBT with environmental variables and the relationships between MAP and MAAT for various alkaline soil data sets (**a–c**: integrated Chinese alkaline soils; **d–f**: alkaline soils in the USA (De Jonge et al., 2014); **g–i**: alkaline soils in the Iberian Peninsula; Menges et al., 2014). Solid circles in **(a–c)** represent soils newly collected in this study, while circles are published data from Yang et al. (2012, 2014a) and Xie et al. (2012).

3.4 Implications for palaeorainfall reconstruction on the CLP

The significant ($p < 0.01$) correlation between CBT and MAP in Chinese alkaline soils implies that the CBT index may be a useful tool for palaeorainfall reconstruction in LPS. When only CLP soils collected in this study were considered, the positive CBT–MAP correlation exhibits an obvious improvement (Fig. 7a):

$$\mathrm{CBT} = -0.0021 \times \mathrm{MAP} + 1.7 (r = -0.93,\ p < 0.01,\ n = 37). \quad (6)$$

We apply this initial calibration on three LPSs with published bGDGT data covering the past 70 ka, in order to validate the CBT index as a palaeorainfall proxy on the CLP. The residual errors of the estimated MAP are < 127 mm, with a RMSE of 50 mm and without following a clear trend with MAP (Fig. 7b). Analytically, the standard deviation for CBT is 0.01, equivalent to 6 mm of MAP, indicating that palaeorainfall estimates can be obtained with high analytical reproducibility. Located from west to east on the southern CLP, the three LPSs are the Yuanbao (Fig. 8a; Jia et al., 2013), Lantian (Fig. 8b; Gao et al., 2012), and Mangshan (Fig. 8c; Peterse et al., 2014) sections, respectively. The CBT-derived MAP records exhibit pronounced precession-driven variation in rainfall amount at the three sites. Within dating uncertainties, the fluctuations of each record resemble the speleothem δ^{18}O record from the Hulu (Wang et al., 2001) and Sanbao (Wang et al., 2008) caves in southeastern China (Fig. 8d), which are widely regarded as a robust record for the EASM intensity, predominantly for monsoon precipitation (Peterse et al., 2014). All these records indicate that rainfall amount was highest during marine isotope stage (MIS) 1, relatively higher during MIS 3, and lowest during MIS 2 and probably MIS 4. Overall, the consistency of the CBT-inferred MAP records with the independent speleothem δ^{18}O monsoon rainfall record (Wang et al., 2001, 2008) strongly supports the CBT index as a palaeorainfall proxy on the CLP.

According to the preliminary modern CBT–MAP calibration, the minimum MAP values for the three sites (559 mm, 726 mm, and 616 mm for Yuanbao, Lantian, and Mang-

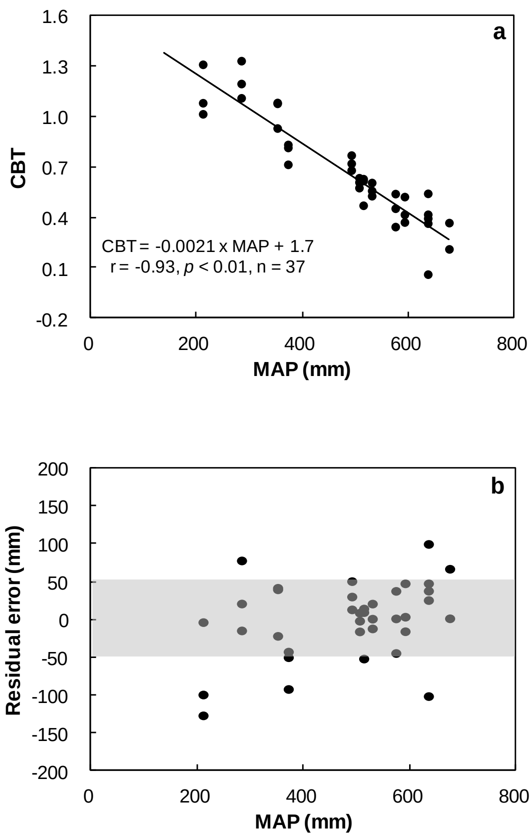

Figure 7. (a) Calibration plot of CBT vs. local MAP of surface CLP soils collected in this study. **(b)** MAP vs. residual MAP (meteorological MAP – estimated MAP using the surface soil calibration in the CLP). Grey shade marks the data within the RMSE (50 mm).

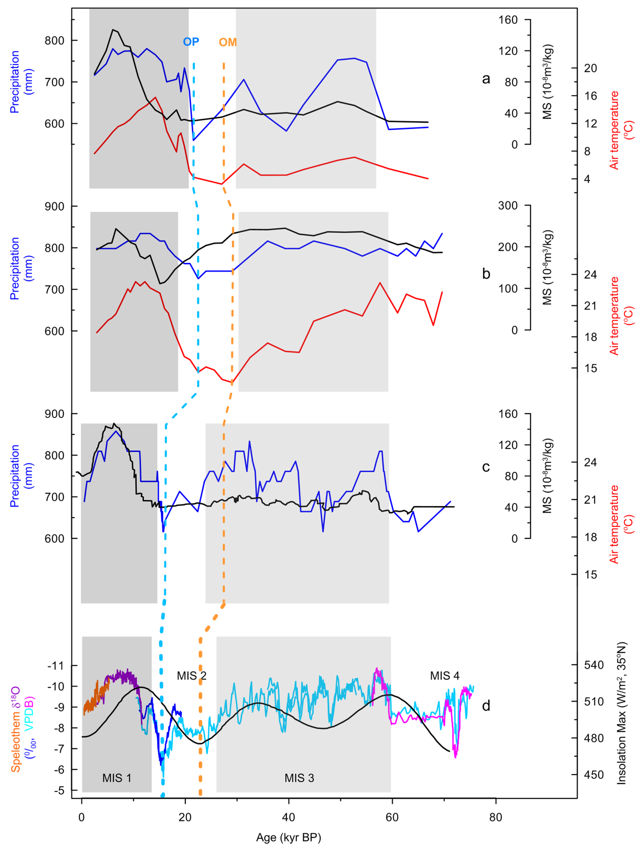

Figure 8. Comparison of variations in CBT-inferred MAP, bGDGT-derived temperature and magnetic susceptibility (MS) records of three LPS sections **(a, b, c)** with speleothem-based EASM record (Wang et al., 2001, 2008) and local insolation (Huybers, 2006) **(d)**. The three LPS sections are from Yuanbao (**a**, Jia et al., 2013), Lantian (**b**, Gao et al., 2012) and Mangshan (**c**, Peterse et al., 2014), respectively. The grey shade, light grey shade, blue dashed line, and orange dashed line indicate MIS 1, MIS 3, onset of precipitation enhancement (OP), and onset of deglacial warming (OM), respectively.

shan, respectively) since the last glacial occurred at the Last Glacial Maximum (LGM), while the maximum values (780 mm, 834 mm, and 858 mm for Yuanbao, Lantian, and Mangshan, respectively) were reached during the Holocene, showing an overall ca. 200 mm enhancement in MAP on average during the transitional deglacial period in the southern CLP. Moreover, the maximum and minimum values of reconstructed MAP for the Yuanbao LPS are much lower than those of Lantian and Mangshan LPSs. This is in agreement with the modern isohyet's pattern showing a decreasing MAP from east to west CLP (Fig. 1). However, these quantitative results based on CBT data measured by different laboratories should be interpreted with caution, since recent round-robin studies with dozens of laboratories have shown that GDGT indices may vary due to differences in interlaboratory instrumental characteristics (Schouten et al., 2013b).

The CBT–MAP relationship in alkaline soils provides an empirical basis for the direct reconstruction of palaeorainfall based on the CBT index on the CLP instead of linking them via pH. Previously, the CBT index has been used successfully as a qualitative indicator of past precipitation in tropical Africa, given that large-scale changes in soil pH reflect changes in regional precipitation (Weijers et al., 2007b, and references therein). Recently, Peterse et al. (2014) proposed that the comparison of CBT-derived pH (likely precipitation-induced) and bGDGT-derived temperature in the LPS might enable us to further assess the relative timing and magnitude of hydrological and thermal changes in continental East Asia, independently of potential biases associated with age model uncertainties. However, the reconstructed pH is unexpectedly higher in palaeosols than in loess (Jia et al., 2013; Peterse et al., 2014), resulting in an inference of lower precipitation when palaeosols formed according to the assumption of Weijers et al. (2007b) that higher palaeosoil pH is related to drier conditions. In this study, we show that the CBT index possibly correlates directly with precipitation intensity, providing an explanation for the perplexing results of previous studies (Jia et al., 2013; Peterse et al., 2014). In view of the great potential of bGDGTs in reconstructing continental air temperature (Weijers et al., 2007a; Peterse et al., 2012; De Jonge et al., 2014; Yang et al., 2014a), the application of the CBT index derived from the same suite of lipids as a palaeorainfall proxy might be particularly promising on the CLP.

3.5 Temperature proxies based on bGDGTs

The MBT' / CBT-derived MAATs are consistently lower than the meteorological MAAT for the Chinese alkaline soils (Fig. 9a). This is in agreement with a number of recent investigations which observed that the MBT' / CBT proxy underestimates MAAT in arid and alkaline conditions (Peterse et al., 2012; Dirghangi et al., 2013; Menges et al., 2014; Yang et al., 2014a). Such a "cold bias" of MBT' / CBT-derived MAAT in arid soils can be attributed in part to an enhanced hydrological (MAP) influence on MBT' (Peterse et al., 2012; Dirghangi et al., 2013; Menges et al., 2014). For this data set, the MBT' values are indeed generally lower than those for the globally distributed soils (Peterse et al., 2012) with the same MAAT (Fig. 9b). Recently, De Jonge et al. (2014) further suggest the underestimation of MAAT for arid soils may be forthcoming from the fact that higher pH (induced by more aridity; Xie et al., 2012) could increase the production of 6-methyl bGDGTs. When using the traditional cyano HPLC column, the co-eluting 6-methyl bGDGTs increase the peak areas of the "normal" 5-methyl bGDGTs for IIa, IIb, IIc and IIIa. This would decrease the calculated MBT' and reconstructed temperature, whereas it is actually caused by a higher pH rather than lower temperature. Moreover, the insensitivity of CBT to soil pH variation in alkaline soils might also be responsible for the "cold bias" of MBT' / CBT-derived MAAT. Actually, when applying the global MBT' / pH MAAT calibration (Peterse et al., 2012), in which CBT is replaced by measured soil pH, we observed that the reconstructed temperature for the Chinese alkaline soil data set is improved (Fig. 9a). Overall, therefore, due to the problem in both MBT' and CBT indices, the MBT' / CBT temperature proxy should be applied with caution for quantitative palaeotemperature reconstructions in soils from arid–subhumid regions.

Given the uncertainty in the MBT' / CBT proxy in arid/semiarid regions, Yang et al. (2014a) proposed an alternative transfer function (i.e. the Chinese SSM calibration) for temperature reconstruction based on the fractional abundances of bGDGTs. According to this calibration, the reconstructed MAAT compares favourably to meteorological MAAT for the Chinese alkaline soil data set (Fig. 9a), with a mean difference of 1.8 °C and no obvious bias. Therefore, the Chinese SSM calibration might be generally more applicable for quantitative palaeotemperature reconstructions in alkaline soils from arid–subhumid China, in particular on the CLP.

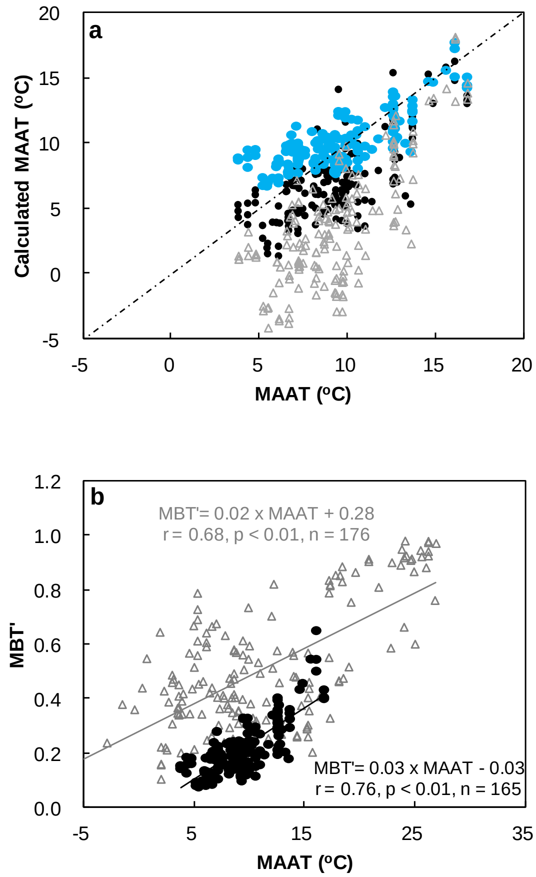

Figure 9. Linear regression plots of **(a)** reconstructed MAAT vs. meteorological MAAT and **(b)** MBT' vs. meteorological MAAT. In **(a)**, calculated MAAT based on the global MBT' / CBT calibration and MBT' / pH calibration (Peterse et al., 2012) is indicated in grey triangles and dark solid circles, respectively, while calculated MAAT based on the Chinese SSM calibration (Yang et al., 2014a) is indicated in blue solid circles. In **(b)**, grey triangles indicate data compiled by Peterse et al. (2012) while solid circles represent Chinese alkaline soil samples (97 from this study and 78 from Yang et al., 2012; Xie et al., 2012; and Yang et al., 2014a).

4 Summary

In this study, we have investigated the environmental controls on the distribution of bGDGTs for surface soils on the CLP and in other alkaline soils from arid–subhumid China. In contrast to most previous studies covering a large range of soil pH values, no obvious relationship was observed between soil pH and CBT for our alkaline soil data set. Further examination of other environmental factors showed that CBT is best correlated with SWC and MAP, indicating that soil moisture might have played an important role on the cyclization ratio of bGDGTs in alkaline soils in the water-limited environment.

A preliminary regional calibration of MAP and CBT was established by using 37 well-drained natural soils on the CLP

(CBT = −0.0021 × MAP + 1.7). With a RMSE of 50 mm for the estimated MAP, this correlation might be useful for inferring past rainfall variation in this climatologically important region. According to this calibration, variation in reconstructed MAP for the past 70 ka based on three sets of published bGDGT data on the CLP (Yuanbao: Jia et al., 2013; Lantian: Gao et al., 2012; Mangshan: Peterse et al., 2014) is in agreement with the speleothem δ^{18}O record, within age model uncertainties. The combination of the CBT rainfall indicator with the bGDGT temperature proxy derived from the same suite of lipids tells a similar story of the lag of monsoon precipitation relative to continental temperature at the three sites, independent of chronology. Moreover, the maximum and minimum values of reconstructed MAP for the drier Yuanbao section on the eastern CLP are systematically lower than those of the more humid Lantian and Mangshan sections on the western CLP. This evidence collectively support the CBT index as a promising new palaeorainfall proxy on the CLP, although further research is needed to explore the detailed mechanisms for the negative CBT–MAP relationship in alkaline soils from arid–subhumid regions.

The Supplement related to this article is available online at doi:10.5194/bg-11-6755-2014-supplement.

Acknowledgements. We would like to thank Hui Zhao for help in the preparation of figures. The China Meteorological Data Sharing Service System is thanked for providing free climatic data. We also thank the anonymous reviewers for their constructive comments. This research was financially supported by the key deployment project from the Chinese Academy of Sciences (no. KZZD-EW-04-06), the national key funds of China (no. 2013CB955901), the Chinese Academy of Sciences (no. XDA05120402), National Natural Science Foundation of China grants no. 41030211 (WL) and 41373072 (CLZ), and the open fund of SKLLQG CAS (no. Y352000317). LC-MS analysis was performed in the State Key Laboratory of Marine Geology through the National Thousand Talents Program at Tongji University (CLZ).

Edited by: A. Neftel

References

An, Z.: The history and variability of the East Asian paleomonsoon climate, Quaternary Sci. Rev., 19, 171–187, 2000.

An, Z., Huang, Y., Liu, W., Guo, Z., Clemens, S., Li, L., Prell, W., Ning, Y., Cai, Y., Zhou, W., Lin, B., Zhang, Q., Cao, Y., Qiang, X., Chang, H., and Wu, Z.: Multiple expansions of C4 plant biomass in East Asia since 7 Ma coupled with strengthened monsoon circulation, Geology, 33, 705–708, 2005.

Booth, I. R.: Regulation of cytoplasmic pH in bacteria, Microbiol. Rev., 359–378, 1985.

De Jonge, C., Hopmans, E. C., Stadnitskaia, A., Rijpstra, W. I. C., Hofland, R., Tegelaar, E., and Sinninghe Damsté, J. S.: Identification of novel penta- and hexamethylated branched glycerol dialkyl glycerol tetraethers in peat using HPLC-MS^2, GC-MS and GC-SMB-MS, Org. Geochem. 54, 78–82, 2013.

De Jonge, C., Hopmans, E. C., Zell, C. I., Kim, J.-H., Schouten, S., and Sinninghe Damsté, J. S.: Occurrence and abundance of 6-methyl branched glycerol dialkyl glycerol tetraethers in soils: Implications for palaeoclimate reconstruction, Geochim. Cosmochim. Acta, 141, 97–112, 2014.

Ding, Y.: Monsoons over China, Kluwer Academics Publishers, Dordrecht, 1994.

Ding, Z., Yang, S., Sun, J., and Liu, T.: Iron geochemistry of loess and red clay deposits in the Chinese Loess Plateau and implications for long-term Asian monsoon evolution in the last 7.0 Ma, Earth Planet. Sci. Lett., 185, 99–109, 2001.

Dirghangi, S. S., Pagani, M., Hren, M. T., and Tipple, B. J.: Distribution of glycerol dialkyl glycerol tetraethers in soils from two environmental transects in the USA, Org. Geochem., 59, 49–60, 2013.

Gao, L., Nie, J., Clemens, S., Liu, W., Sun, J., Zech, R., and Huang, Y.: The importance of solar insolation on the temperature variations for the past 110 kyr on the Chinese Loess Plateau, Palaeogeogr. Palaeoclimatol. Palaeoecol., 317–318, 128–133, 2012.

Guo, Z., Ruddiman, W. F., Hao, Q., Wu, H., Qiao, Y., Zhu, R., Peng, S., Wei, J., Yuan, B., and Liu, T.: Onset of Asian desertification by 22 Myr ago inferred from loess deposits in China, Nature, 416, 159–163, 2002.

Heller, F. and Liu, T.: Magnetostratigraphical dating of loess deposits in China, Nature, 300, 431–433, 1982.

Hopmans, E. C., Schouten, S., Pancost, R. D., van der Meer, M. T. J., and Sinninghe Damsté, J. S.: Analysis of intact tetraether lipids in archaeal cell material and sediments by high performance liquid chromatography/atmospheric pressure chemical ionization mass spectrometry, Rapid Commun. Mass Spectrom., 14, 585–589, 2000.

Hopmans, E. C., Weijers, J. W. H., Schefuss, E., Herfort, L., Sinninghe Damsté, J. S., and Schouten, S.: A novel proxy for terrestrial organic matter in sediments based on branched and isoprenoid tetraether lipids, Earth Planet. Sci. Lett., 224, 107–116, 2004.

Huguet, A., Fosse, C., Metzger, P., Fritsch, E., and Derenne, S.: Occurrence and distribution of extractable glycerol dialkyl glycerol tetraethers in podzols, Org. Geochem., 41, 291–301, 2010.

Huguet, C., Hopmans, E. C., Febo-Ayala, W., Thompson, D. H., Sinninghe Damsté, J. S., and Schouten, S.: An improved method to determine the absolute abundance of glycerol dibiphytanyl glycerol tetraether lipids, Org. Geochem., 37, 1036–1041, 2006.

Huybers, P.: Early Pleistocene glacial cycles and the integrated summer insolation forcing, Science, 313, 508–511, 2006.

Jia, G., Rao, Z., Zhang, J., Li, Z., and Chen, F.: Tetraether biomarker records from a loessepaleosol sequence in the western Chinese Loess Plateau, Front. Microbiol., 4, 199, doi:10.3389/fmicb.2013.00199, 2013.

Li, G., Sheng, X., Chen, J., Yang, J., and Chen, Y.: Oxygen-isotope record of paleorainwater in authigenic carbonates of Chinese loess-paleosol sequences and its paleoclimatic significance, Palaeogeogr. Palaeoclimatol. Palaeoecol., 245, 551–559, 2007.

Li, T. and Li, G.: Incorporation of trace metals into microcodium as novel proxies for paleo-precipitation, Earth Planet. Sci. Lett., 386, 34–40, 2014.

Liu, T.: Loess and the Environment, China Ocean Press, Beijing, 1985.

Liu, T. and Ding, Z.: Chinese loess and the paleomonsoon, Annu. Rev. Earth. Pl. Sc., 26, 111–145, 1998.

Liu, W. and Huang, Y.: Compound specific D/H ratios and molecular distributions of higher plant leaf waxes as novel paleoenvironmental indicators in the Chinese Loess Plateau, Org. Geochem., 36, 851–860, 2005.

Liu, W., Feng, X., Ning, Y., Zhang, Q., Cao, Y., and An, Z.: δ^{13}C variation of C3 and C4 plants across an Asian monsoon rainfall gradient in arid northwestern China, Global Change Biol., 11, 1094–1100, 2005a.

Liu, W., Huang, Y., An, Z., Clemens, S. C., Li, L., Prell, W. L., and Ning, Y.: Summer monsoon intensity controls C4/C3 plant abundance during the last 35 ka in the Chinese Loess Plateau: carbon isotope evidence from bulk organic matter and individual leaf waxes, Palaeogeogr. Palaeoclimatol. Palaeoecol., 220, 243–254, 2005b.

Liu, W., Ning, Y., An, Z., Wu, Z., Lu, H., and Cao, Y.: Carbon isotopic composition of modern soil and paleosol as a response of vegetation change in Loess Plateau, Sci. China Earth Sci., 48, 93–99, 2005c.

Liu, W., Yang, H., Sun, Y., and Wang, X.: δ^{13}C values of loess total carbonate: A sensitive proxy for Asian summer monsoon in arid northwestern margin of the Chinese loess plateau, Chem. Geol., 284, 317–322, 2011.

Liu, W., Wang, H., Zhang, C. L., Liu, Z., and He, Y.: Distribution of glycerol dialkyl glycerol tetraether lipids along an altitudinal transect on Mt. Xiangpi, NE Qinghai-Tibetan Plateau, China, Org. Geochem., 57, 76–83, 2013.

Loomis, S., Russell, J., and Sinninghe Damsté, J. S.: Distributions of branched GDGTs in soils from western Uganda and implications for a lacustrine paleothermometer, Org. Geochem., 42, 739–751, 2011.

Lu, H., Wu, N., Yang, X., Jiang, H., Liu, K., and Liu, T.: Phytoliths as quantitative indicators for the reconstruction of past environ mental conditions in China I: phytolith-based transfer functions, Quaternary Sci. Rev., 25, 945–959, 2006.

Lu, H., Wu, N., Liu, K., Jiang, H., and Liu, T.: Phytoliths as quantitative indicators for the reconstruction of past environmental conditions in China II: palaeoevironmental reconstruction in the Loess Plateau, Quaternary Sci. Rev., 26, 759–772, 2007.

Maher, B., Thompson, R., and Zhou, L.: Spatial and temporal reconstructions of changes in the Asian palaeomonsoon: a new mineral magnetic approach, Earth Planet. Sci. Lett., 125, 461–471, 1994.

Menges, J., Huguet, C., Alcañiz, J. M., Fietz, S., Sachse, D., and Rosell-Melé, A.: Influence of water availability in the distributions of branched glycerol dialkyl glycerol tetraether in soils of the Iberian Peninsula, Biogeosciences, 11, 2571–2581, doi:10.5194/bg-11-2571-2014, 2014.

Ning, Y., Liu, W., and An, Z.: A 130-ka reconstruction of precipitation on the Chinese Loess Plateau from organic carbon isotopes, Palaeogeogr. Palaeoclimatol. Palaeoecol., 270, 59–63, 2008.

Oppermann, B. I., Michaelis, W., Blumenberg, M., Frerichs, J., Schulz, H.-M., Schippers, A., Beaubien, S. E., and Krüger, M.: Soil microbial community changes as a result of long-term exposure to a natural CO_2 vent, Geochim. Cosmochim. Acta, 74, 2697–2716, 2010.

Pancost, R. D. and Sinninghe Damsté, J. S.: Carbon isotopic compositions of prokaryotic lipids as tracers of carbon cycling in diverse settings, Chem. Geol., 195, 29–58, 2003.

Peterse, F., Kim, J.-H., Schouten, S., Klitgaard Kristensen, D., Koç, N., and Sinninghe Damsté, J. S.: Constraints on the application of the MBT/CBT paleothermometer in high latitude environments (Svalbard, Norway), Org. Geochem., 40, 692–699, 2009a.

Peterse, F., van der Meer, M. T. J., Schouten, S., Jia, G., Ossebaar, J., Blokker, J., and Sinninghe Damsté, J. S.: Assessment of soil n-alkane αD and branched tetraether membrane lipid distributions as tools for paleoelevation reconstruction, Biogeosciences, 6, 2799–2807, doi:10.5194/bg-6-2799-2009, 2009b.

Peterse, F., Nichol, G., Schouten, S., and Sinninghe Damsté, J. S.: Influence of soil pH on the abundance and distribution of core and intact polar lipid-derived branched GDGTs in soil, Org. Geochem., 41, 1171–1175, 2010.

Peterse, F., Prins, M. A., Beets, C. J., Troelstra, S. R., Zheng, H., Gu, Z., Schouten, S., and Sinninghe Damsté, J. S.: Decoupled warming and monsoon precipitation in East Asia over the last deglaciation, Earth Planet. Sc Lett., 301, 256–264, 2011.

Peterse, F., van der Meer, J., Schouten, S., Weijers, J. W. H., Fierer, N., Jackson, R. B., Kim, J.-H., and Sinninghe Damsté, J. S.: Revised calibration of the MBT-CBT paleotemperature proxy based on branched tetraether membrane lipids in surface soils, Geochim. Cosmochim. Acta, 96, 215–229, 2012.

Peterse, F., Martínez-García, A., Zhou, B., Beets, C. J., Prins, M. A., Zheng, H., and Eglinton, T. I.: Molecular records of continental air temperature and monsoon precipitation variability in East Asia spanning the past 130,000 years, Quaternary Sci. Rev., 83, 1–7, 2014.

Porter, S. C.: Chinese loess record of monsoon climate during the last glacial-interglacial cycle, Earth-Sci. Rev., 54, 115–128, 2001.

Qiang, X., An, Z., Song, Y., Chang, H., Sun, Y., Liu, W., Ao, H., Dong, J., Fu, C., Wu, F., Lu, F., Cai, Y., Zhou, W., Cao, J., Xu, X., and Ai, L.: New eolian red clay sequence on the western Chinese Loess Plateau linked to onset of Asian desertification about 25 Ma ago, Sci. China Earth Sci., 54, 136–144, 2011.

Rao, Z., Chen, F., Cheng, H., Liu, W., Wang, G., Lai, Z., and Bloemendal, J.: High-resolution summer precipitation variations in the western Chinese Loess Plateau during the last glacial, Sci. Rep., 3, 2785, doi:10.1038/srep02785, 2013.

Schoon, L., de Kluijver, A., Middelburg, J. J., Downing, J. A., Sinninghe Damsté, J. S., and Schouten, S.: Influence of lake water pH and alkalinity on the distribution of core and intact polar branched glycerol dialkyl glycerol tetraethers (GDGTs) in lakes, Org. Geochem., 60, 72–82, 2013.

Schouten, S., Huguet, C., Hopmans, E. C., and Sinninghe Damsté, J. S.: Improved analytical methodology of the TEX_{86} palaeothermometry by high performance liquid chromatography/atmospheric pressure chemical ionization-mass spectrometry, Anal. Chem., 79, 2940–2944, 2007.

Schouten, S., Hopmans, E. C., and Sinninghe Damsté, J. S.: The Org. Geochem., of glycerol dialkyl glycerol tetraether lipids: a review, Org. Geochem., 54, 19–61, 2013a.

Schouten, S., Hopmans, E. C., Rosell-Melé, A., Pearson, A., Adam, P., Bauersachs, T., Bard, E., Bernasconi, S., Bianchi, T. S., Brocks, J. J., Truxal-Carlson, L., Castañeda, I. S., Dutta, K., Eglinton, T., Fosse, C., Grice, K., Hinrichs, K. E., Huang, Y., Huguet, A., Huguet, C., Hurley, S., Ingalls, A., Jia, G., Keely, B., Knappy, C., Lincoln, S., Lipp, J., Mangelsdorf, K., Martinez-Garcia, A., van-der-Meer, J., Ménot-Combes, G., Mets, A., Mollenhauer, G., Ohkouchi, N., Ossebaar, J., Pagani, M., Pancost, R. D., Pearson, E. J., Peterse, F., Reichart,G. J., Schaeffer, P., Schmitt, G., Selver, A. D., Shah, S. R., Smith, R. W., Smittenberg, R., Takano, Y., Talbot, H. M., Taylor, K. W. R., Tarozo, R., Van-Dongen, B. E., Van-Mooy, B. A. S., Weijers, J. W. H., Werne, J. P., Woltering, M., Xie, S., Yamamoto, M., Yang, H., Zhang, C., Zhao, M., and Sinninghe Damsté, J. S.: An interlaboratory study of TEX_{86} and BIT analysis of sediments, extracts and standard mixtures, Geochem. Geophy. Geosy., 14, 5263–5285, doi:10.1002/2013GC004904, 2013b.

Sinninghe Damsté, J. S., Hopmans, E. C., Pancost, R. D., Schouten, S., and Geenevasen, J. A. J.: Newly discovered non-isoprenoid dialkyl diglycerol tetraether lipids in sediments. Journal of the Chemical Society, Chem. Commun., 23, 1683–1684, 2000.

Sinninghe Damsté, J. S., Ossebaar, J., Schouten, S., and Verschuren, D.: Altitudinal shifts in the distribution of branched tetraether lipids in soils from Mt. Kilimanjaro (Tanzania): implications for the MBT/CBT continental palaeothermometer, Org. Geochem., 39, 1072–1076, 2008.

Sinninghe Damsté, J. S., Rijpstra, W. I. C., Hopmans, E. C., Weijers, J. W. H., Foesel, B. U., Overmann, J., and Dedysh, S. N.: 13,16-Dimethyl octacosanedioic acid (iso-diabolic acid): a common membrane-spanning lipid of Acidobacteria subdivisions 1 and 3, Appl. Environ. Microb., 77, 4147–4154, 2011.

Speelmans, G., Poolman, B., and Konings, W. N.: Na^{+} as coupling ion in energy transduction in extremophilic bacteria and archaea, World J. Microb. Biot., 11, 58–70, 1995.

Sun, Q., Chu, G., Liu, M., Xie, M., Li, S., Ling, Y., Wang, X., Shi, L., Jia, G., and Lu, H.: Distributions and temperature dependence of branched glycerol dialkyl glycerol tetraethers in recent lacustrine sediments from China and Nepal, J. Geophys. Res., 116, G01008, doi:10.1029/2010JG001365, 2011.

Sun, Y., Clemens, S. C., An, Z., and Yu, Z.: Astronomical timescale and palaeoclimatic implication of stacked 3.6-Ma monsoon records from the Chinese Loess Plateau, Quaternary Sci. Rev., 25, 33–48, 2006.

ter Braak, C. J. F.: Canoco-a FORTRAN program for canonical community ordination by (partial) (detrended) (canonical) correspondence analysis, principal components analysis and redundancy analysis (version 2.1), Technical Rep. LWA-88-02, GLW, Wageningen, 95 pp., 1988.

ter Braak, C. J. F. and Prentice, I. C.: A theory of gradient analysis, Adv. Ecol. Res., 18, 271–317, 1988.

ter Braak, C. J. F. and Smilauer, P.: CANOCO reference manual and Canodraw for windows users guide: Software for canonical community ordination (version 4.5), Microcomputer Power, Ithaca, NY, USA, 500 pp., 2002.

Tierney, J. E. and Russell, J. M.: Distributions of branched GDGTs in a tropical lake system: Implications for lacustrine application of the MBT/CBT palaeoproxy, Org. Geochem., 40, 1032–1036, 2009.

Tierney, J. E., Schouten, S., Pitcher, A., Hopmans, E. C., and Sinninghe Damsté, J. S.: Core and intact polar glycerol dialkyl glycerol tetraethers (GDGTs) in Sand Pond, Warwick, Rhode Island (USA): Insights into the origin of lacustrine GDGTs, Geochim. Cosmochim. Acta, 77, 561–581, 2012.

Wang, H., Liu, W., Zhang, C. L., Wang, Z., Wang, J., Liu, Z., and Dong, H.: Distribution of glycerol dialkyl glycerol tetraethers in surface sediments of Lake Qinghai and surrounding soil, Org. Geochem., 47, 78–87, 2012.

Wang, H., Liu, W., Zhang, C., Liu, Z., and He, Y.: Branched and isoprenoid tetraether (BIT) index traces water content along two marsh-soil transects surrounding Lake Qinghai: Implications for paleo-humidity variation, Org. Geochem., 59, 79–81, 2013.

Wang, Y., Cheng, H., Edwards, R. L., An, Z., Wu, J., Shen, C., and Dorale, J. A.: A high-resolution absolute-dated Late Pleistocene monsoon record from Hulu Cave, China, Science, 294, 2345–2348, 2001.

Wang, Y., Cheng, H., Edwards, R., Kong, X., Shao, X., Chen, S., Wu, J., Jiang, X., Wang, X., and An, Z.: Millennial- and orbital-scale changes in the East Asian monsoon over the past 224,000 years, Nature, 451, 1090–1093, 2008.

Weijers, J. W. H., Schouten, S., Spaargaren, O. C., and Sinninghe Damsté, J. S.: Occurrence and distribution of tetraether membrane in soils: implications for the use of the BIT index and the TEX86 SST proxy, Org. Geochem., 37, 1680–1693, 2006a.

Weijers, J. W. H., Schouten, S., Geenevasen, J. A. J., David, O. R. P., Coleman, J., Pancost, R. D., and Sinninghe Damsté, J. S.: Membrane lipids of mesophilic anaerobic bacteria thriving in peats have typical archaeal traits, Environ. Microb., 8, 648–657, 2006b.

Weijers, J. W. H., Schouten, S., van Den Donker, J. C., Hopmans, E. C., and Sinninghe Damsté, J. S.: Environmental controls on bacterial tetraether membrane lipid distribution in soils, Geochim. Cosmochim. Acta, 71, 703–713, 2007a.

Weijers, J. W. H., Schefuss, E., Schouten, S., and Sinninghe Damsté, J. S.: Coupled thermal and hydrological evolution of tropical Africa over the last deglaciation, Science, 315, 1701–1704, 2007b.

Weijers, J. W. H., Wiesenberg, G. L. B., Bol, R., Hopmans, E. C., and Pancost, R. D.: Carbon isotopic composition of branched tetraether membrane lipids in soils suggest a rapid turnover and a heterotrophic life style of their source organism(s), Biogeosciences, 7, 2959–2973, doi:10.5194/bg-7-2959-2010, 2010.

Xia, D., Jia, J., Wei, H., Liu, X., Ma, J., Wang, X., and Chen, F.: Magnetic properties of surface soils in the Chinese Loess Plateau and the adjacent Gobi areas, and their implication for climatic studies, J. Arid Environ., 78, 73–79, 2012.

Xie, S., Pancost, R. D., Chen, L., Evershed, R. P., Yang, H., Zhang, K., Huang, J., and Xu, Y.: Microbial lipid records of highly alkaline deposits and enhanced aridity associated with significant uplift of the Tibetan Plateau in the Late Miocene, Geology, 40, 291–294, 2012.

Yang, H., Ding, W., Wang, J., Jin, C., He, G., Qin, Y., and Xie, S.: Soil pH impact on microbial tetraether lipids and terrestrial input index (BIT) in China, Sci. China Earth Sci., 55, 236–245, 2012.

Yang, H., Pancost, R. D., Dang, X., Zhou, X., Evershed, R. P., Xiao, G., Tang, C., Gao, L., Guo, Z., and Xie, S.: Correlations between microbial tetraether lipids and environmental variables in Chinese soils: Optimizing the paleo-reconstructions in semi-arid and arid regions, Geochim. Cosmochim. Acta, 126, 49–69, 2014a.

Yang, H., Pancost, R. D., Tang, C., Ding, W., Dang, X., and Xie, S.: Distributions of isoprenoid and branched glycerol dialkanol diethers in Chinese surface soils and a loess–paleosol sequence: Implications for the degradation of tetraether lipids, Org. Geochem., 66, 70–79, 2014b.

Zhang, C. L. Wang, J., Wei, Y., Zhu, C., Huang, L., and Dong, H.: Production of branched tetraether lipids in the lower Pearl River and estuary: effects of extraction methods and impact on bGDGT proxies, Front. Microbiol., 2, 274, doi:10.3389/fmicb.2011.00274, 2012.

Zhang, Z., Zhao, M., Lu, H., and Faiia, A. M.: Lower temperature as the main cause of C4 plant declines during the glacial periods on the Chinese Loess Plateau, Earth Planet. Sci. Lett., 214, 467–481, 2003.

Zhang, Z., Zhao, M., Eglinton, G., Lu, H., and Huang, C.: Leaf wax lipids as paleovegetational and paleoenvironmental proxies for the Chinese Loess Plateau over the last 170 kyr, Quaternary Sci. Rev., 25, 575–594, 2006.

Zhou, L., Oldfield, F., Wintle, A. G., Robinson, S. G., and Wang, J.: Partly pedogenic origin of magnetic variations in Chinese loess, Nature, 346, 737–739, 1990.